

The Proapoptotic G41S Mutation to Human Cytochrome *c* Alters the Heme Electronic Structure and Increases the Electron Self-Exchange Rate

Matthew D. Liptak,[†] Robert D. Fagerlund,[‡] Elizabeth C. Ledgerwood,[‡] Sigurd M. Wilbanks,[‡] and Kara L. Bren^{*,†}

[†]Department of Chemistry, University of Rochester, Rochester, New York 14627, United States

[‡]Department of Biochemistry, University of Otago, Dunedin, New Zealand

S Supporting Information

ABSTRACT: The naturally occurring G41S mutation to human (*Hs*) cytochrome (*cyt*) *c* enhances apoptotic activity based upon previous *in vitro* and *in vivo* studies, but the molecular mechanism underlying this enhancement remains unknown. Here, X-ray crystallography, nuclear magnetic resonance (NMR) spectroscopy, and density functional theory (DFT) calculations have been used to identify the structural and electronic differences between wild-type (WT) and G41S *Hs* *cyt c*. S41 is part of the hydrogen bonding network for propionate 7 of heme pyrrole ring A in the X-ray structure of G41S *Hs* *cyt c* and, compared to WT, G41S *Hs* *cyt c* has increased spin density on pyrrole ring C and a faster electron self-exchange rate. DFT calculations illustrate an electronic mechanism where structural changes near ring A can result in electronic changes at ring C. Since ring C is part of the solvent-exposed protein surface, we propose that this heme electronic structure change may ultimately be responsible for the enhanced proapoptotic activity of G41S *Hs* *cyt c*.

In addition to its well described role in the mitochondrial electron transport chain, human (*Hs*) cytochrome (*cyt*) *c* is active in the intrinsic apoptotic pathway where it is released into the cytosol and interacts with apoptosis protease activating factor-1 (Apaf-1). This interaction promotes apoptosome assembly, caspase activation, and, ultimately, triggers cell death. The G41S mutant, which was previously identified in patients diagnosed with a form of mild autosomal dominant thrombocytopenia consistent with enhanced apoptotic activity *in vivo*, was the first mutation identified in *Hs* *cyt c* and is currently the only variant of *Hs* *cyt c* known to have an enhanced ability to activate caspases *in vitro*.¹ The G41S mutation does not appear to affect mitochondrial respiration and the molecular mechanism underlying the enhanced caspase activation remains unknown.

The *in vitro* assay monitors caspase activation in cytosolic extracts, which suggests that the proapoptotic activity of G41S *cyt c* is related to the apoptosome assembly step. A 9.5-Å resolution structure of the human apoptosome was recently reported; the density map is consistent with the presence of folded *cyt c*, but the binding orientation could not be determined unambiguously.²

Nevertheless, researchers have identified several charged surface residues in the vicinity of pyrrole rings A and C that are critical for both *in vitro* and *in vivo* binding and activation of Apaf-1.^{3,4} G41 is not a charged surface residue, but several groups have identified another important factor governing the interaction of *cyt c* and Apaf-1. Only oxidized *cyt c*, and not reduced *cyt c*, promotes apoptosome assembly.⁵ Yet, *cyt c* is rapidly reduced in the cytosol following release from the mitochondria.⁶ In light of this apparent contradiction, we propose that the electronic properties of the heme cofactor are related to the apoptotic activity of *cyt c* and here we present an experimental and theoretical characterization of the redox properties of WT and G41S human *cyt c*.

We collected high resolution X-ray crystallographic diffraction data of reduced G41S *Hs* *cyt c* to identify any structural changes introduced by the mutation. Using data to 1.9 Å, the structure was solved through molecular replacement and refined to an R_{cryst} of 0.17 and R_{free} of 0.20 (Tables S1 and S2). All four copies present in the asymmetric unit display essentially the same structure (PDB ID 3NWV). As seen in other *cyt c* structures, ring C is the most solvent-exposed part of the heme. The G41S mutation displaces residues 41 and 42 approximately 0.4 Å away from Tyr48 which forms the core of the third “omega loop”. Immediately under this “omega loop”, heme propionate 7 is close enough to hydrogen bond with the main-chain amide of residue 41, the hydroxyl of Tyr48, and the side-chain nitrogens of Asn52 and Trp59. In the high resolution crystal structure of reduced tuna *cyt c* (the highest resolution structure available for a reduced homologue of *Hs* *cyt c*), propionate 7 appears to be directly hydrogen bonded to the ϵ -amido group of Arg38.⁷ In contrast, the side chain of Arg38 in G41S *Hs* *cyt c* is in a different conformation and interacts with heme propionate 7 through a pair of ordered water molecules (Figure 1). There are no large-scale structural differences between the X-ray structures of reduced tuna (SCYT) and reduced G41S *Hs* *cyt c* (3NWV), but there is evidence for an altered hydrogen bonding network in the vicinity of propionate 7.

Next, we used nuclear magnetic resonance (NMR) spectroscopy to characterize any electronic changes to the heme cofactor in oxidized *Hs* G41S *cyt c*. Heme substituent ¹H and ¹³C resonances were assigned in oxidized (Fe³⁺) and reduced (Fe²⁺) WT and G41S *Hs* *cyts c* using two-dimensional NMR techniques aided by available heme ¹H and ¹³C assignments for horse *cyt c*,⁹ which

Received: July 16, 2010

Published: December 30, 2010

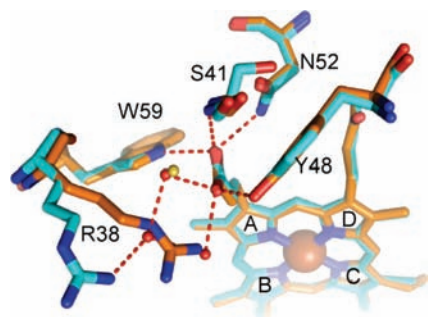


Figure 1. A comparison of the heme *c* environments in the X-ray crystal structures of reduced G41S *Hs cyt c* (3NWV) and reduced tuna *cyt c* (SCYT) with the iron (orange sphere), nitrogen (blue), oxygen (red), G41S *Hs cyt c* carbon (cyan), and tuna *cyt c* carbon (orange) nuclei identified. The porphyrin macrocycle contains four pyrrole rings labeled A–D. Ordered water molecules are shown as small spheres for G41S *Hs cyt c* (red) and reduced tuna (yellow) *cyts c*. The polar interactions of propionate 7 of G41S *Hs cyt c* are indicated by dashed red lines.

Table 1. Experimental and PBE-DFT ^{13}C HFSs (ppm) of Heme *c*

$^{13}\text{C}^a$	experiment			PBE DFT		
	WT ^b	G41S ^b	ΔHFS	P7 ^{-c}	P7H ^c	ΔHFS
1-CH ₃	−32.3	−32.2	0.1	5.6	1.0	−4.6
2-C α	−27.3	−27.0	0.3			
3-CH ₃	−69.4	−70.6	−1.2	−58.4	−126.4	−68.0
4-C α	−75.9	−77.0	−1.2			
5-CH ₃	−38.8	−37.6	1.2	7.3	4.7	−2.6
6-C α	−25.1 ^d	−23.8 ^d	1.3			
7-C α	−57.9 ^d	−57.8 ^d	0.1			
8-CH ₃	−82.2	−82.2	0.0	−115.4	−64.0	51.4

^a Carbons 1 and 2 are attached to ring B, 3 and 4 to ring C, 5 and 6 to ring D, and 7 and 8 to ring A. ^b *Hs cyt c* in 100 mM sodium phosphate (NaP_i) buffer, pH = 7.0, 25 °C. ^c PBE DFT model with deprotonated (P7⁻) and protonated (P7H) propionate 7. ^d HFS derived by subtracting the literature value of the chemical shift in reduced (Fe²⁺) WT *Hs cyt c*.⁸

shares 89% sequence identity with *Hs cyt c*, and reduced WT *Hs cyt c*.⁸ The hyperfine shifts (HFSs) of the ^{13}C nuclei bound to the heme macrocycle were derived by subtracting the chemical shifts of reduced *cyt c* from oxidized *cyt c* (Table 1). The peripheral ^{13}C HFSs of WT *Hs cyt c* are quite similar to those reported for WT horse *cyt c*,⁹ with large negative HFSs on the ^{13}C nuclei attached to rings A and C. In G41S *Hs cyt c*, a larger (more negative) ^{13}C HFS is observed for the nuclei attached to ring C and a smaller (less negative) ^{13}C HFS is observed for the nuclei attached to ring D.

We have used density functional theory (DFT) to investigate the underlying electronic structure responsible for the NMR HFS data. The spin densities and heme methyl ^{13}C HFSs have been calculated for two PBE DFT models that represent the extreme cases of a deprotonated (P7⁻) and a protonated (P7H) propionate 7 side chain using a modified-version of a previously established method (Figure 2).¹⁰ Since a large percentage of the NMR HFSs for nuclei attached to rings B and D arises from thermal population of a low-lying electronic excited state,¹¹ this ground state method will underestimate the ^{13}C HFSs of methyls 1 and 5. Nevertheless, the agreement between the heme methyl ^{13}C HFS

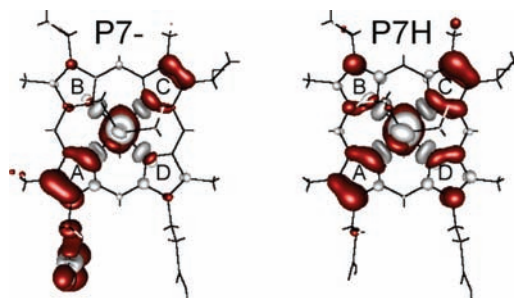


Figure 2. PBE/TZVP DFT-computed unpaired positive (red) and negative (gray) spin densities for the models of heme *c* with a deprotonated (P7⁻) and protonated (P7H) propionate 7 side chain.

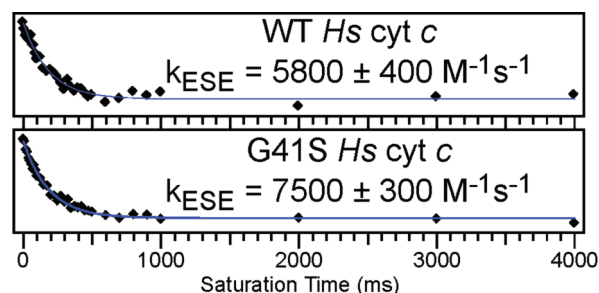


Figure 3. Plots of the intensity of the Met80 $\epsilon\text{-C}^1\text{H}_3$ resonance of reduced (Fe²⁺) *Hs cyt c* and *Hs G41S cyt c* as a function of the saturation time of the Met80 $\epsilon\text{-C}^1\text{H}_3$ resonance of oxidized (Fe³⁺) *cyt c*. Samples were in 100 mM NaP_i buffer, pH = 7.0, 100% D₂O, at 25 °C. The measured intensities (black diamonds) were fit to an exponential decay (blue line) to determine the ESE rate.

data for WT *Hs cyt c* and the P7⁻ DFT model is reasonable with large negative ^{13}C HFSs for the heme methyl groups attached to rings A and C and a more negative HFS for methyl 8 in both cases (Table 1). In the P7H DFT model, the spin density is redistributed onto ring C resulting in a more negative ^{13}C HFS of methyl 3. The spin density can be used to approximate the spatial extent of the singly occupied molecular orbital (SOMO) because spin polarization is minimal in this system (Figures S1 and S2).

The increased SOMO density on ring C in G41S *cyt c* should enhance electronic coupling (H_{AB}) between *Hs cyt c* and external redox partners since ring C is part of the solvent-exposed *Hs cyt c* surface implicated in protein–protein interactions with redox partners.^{12,13} H_{AB} cannot be measured directly, but we can measure the electron self-exchange (ESE) rate, which depends on both H_{AB} and the reorganization energy (λ). The ESE rate between oxidized and reduced *Hs cyt c* was measured in mixed oxidation state NMR samples by time-dependent saturation transfer between the Met80 C^1H_3 resonances of the oxidized and reduced fractions.¹⁴ By analyzing the exponential decay of the ^1H resonance intensity of the reduced fraction as a function of the oxidized fraction saturation time, ESE rate constants of 5800 ± 400 and $7500 \pm 300 \text{ M}^{-1} \text{ s}^{-1}$ were extracted for WT and G41S *cyt c*, respectively (Figure 3). Notably, the ESE rate constant of WT *Hs cyt c* is very similar to that of horse *cyt c* ($5400 \text{ M}^{-1} \text{ s}^{-1}$).¹⁵ Furthermore, the faster ESE rate in G41S *Hs cyt c* is in accord with a larger H_{AB} and/or a smaller λ in G41S *Hs cyt c*.

All of these data can be understood within the framework of a polypeptide-induced perturbation of the heme cofactor elec-

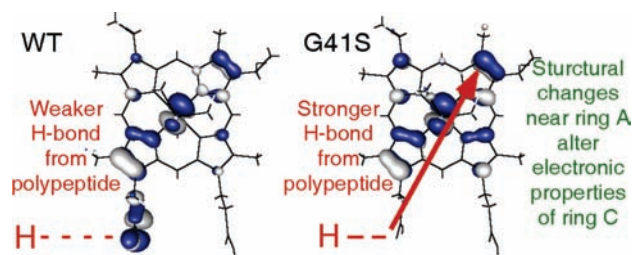


Figure 4. Comparison of DFT computed SOMO for heme with deprotonated (left) and protonated (right) propionate-7. In G41S *Hs* cyt *c*, increased hydrogen-bond donation from the polypeptide to propionate 7 decreases mixing of the propionate orbitals into the SOMO, which results in increased SOMO density on pyrrole ring C. This explains how a mutation near ring A could affect the NMR HFSs of carbons attached to ring C and the ESE rate of *Hs* cyt *c*.

tronic structure. The G41S mutation alters the polypeptide identity and this change is primarily communicated to the heme via the hydrogen bonding network of propionate 7 (Figure 1). Our NMR and DFT data suggest that increased hydrogen bond donation from the polypeptide to propionate 7 in G41S *Hs* cyt *c* would stabilize the $-\text{COO}^-$ π -orbitals, decrease their mixing into the Fe d_{π} -based SOMO, decrease the polarization of the SOMO toward pyrrole ring A, and increase the SOMO density on pyrrole ring C (Figure 4). Since spin polarization is minimal in low-spin Fe(III) heme, increased SOMO density on ring C should correspond to increased spin density on ring C, which explains the larger (more negative) HFSs for methyl 3 and the α -carbon of thioether 4 in G41S *Hs* cyt *c* (Table 1). The increased SOMO density on pyrrole ring C of G41S cyt *c* also provides an explanation for the increased ESE rate (Figure 3), as this electronic structure change is expected to increase H_{AB} .

In summary, previous work has shown that the G41S mutation enhances the apoptotic activity of *Hs* cyt *c*,¹ and the data presented here demonstrate that this mutation also alters the electronic structure of the heme *c* cofactor and increases the ESE rate of the protein. There are at least two explanations for this apparent correlation between the apoptotic activity of *Hs* cyt *c* and the electronic properties of its heme cofactor. First, the enhanced apoptotic activity of G41S *Hs* cyt *c* may be a consequence of this variant's increased ESE rate (Figure 3). The faster ESE rate should correlate to a faster electron transfer rate between *Hs* cyt *c* and redox partners, which would expedite oxidized cyt *c* regeneration from the reduced cyt *c* pool and promote apoptosome assembly.⁵ Alternatively, the electronic changes to the heme cofactor introduced by the G41S mutation may be responsible for enhanced binding and activation of Apaf-1 by *Hs* cyt *c*. The electronic changes should perturb the electrostatic properties of the solvent-exposed pyrrole ring C, which is likely part of the Apaf-1 binding surface based upon the report of diminished caspase activation in the K13A, K72A, and K86A variants of *Hs* cyt *c*.³ To test and differentiate between these two possible explanations for a correlation between the electronic properties of the heme cofactor and apoptosis, future studies will investigate the apoptotic activity, electronic structure, and ESE rate of several *Hs* cyt *c* variants.

■ ASSOCIATED CONTENT

Supporting Information. Experimental details, NMR resonance assignments, PBE DFT-computed MOs, and complete ref 1. This material is available free of charge via the Internet at <http://pubs.acs.org>.

■ AUTHOR INFORMATION

Corresponding Author
bren@chem.rochester.edu

■ ACKNOWLEDGMENT

This work was supported by the NIH (GM63170 to K.L.B. and F32 GM089016 to M.D.L.) and the Marsden Fund (E.C.L.). We acknowledge the University of Rochester Center for Research Computing and the Centre for Protein Research (University of Otago) for resources. We thank Moira Hibbs for technical assistance with protein expression and purification and Prof. Gary Pielak (University of North Carolina) for providing the pBTR(Human Cc) expression vector.

■ REFERENCES

- (1) Morison, I. M.; et al. *Nat. Genet.* **2008**, *40*, 387–389.
- (2) Yuan, S.; Yu, X.; Topf, M.; Ludtke, S. J.; Wang, X.; Akey, C. W. *Structure* **2010**, *18*, 571–583.
- (3) Olteanu, A.; Patel, C. N.; Dedmon, M. M.; Kennedy, S.; Linhoff, M. W.; Minder, C. M.; Potts, P. R.; Deshmukh, M.; Pielak, G. J. *Biochem. Biophys. Res. Commun.* **2003**, *312*, 733–740.
- (4) Hao, Z.; Duncan, G. S.; Chang, C.-C.; Elia, A.; Fang, M.; Wakeham, A.; Okada, H.; Calzascia, T.; Jang, Y.; You-Ten, A.; Yeh, W.-C.; Ohashi, P.; Wang, X.; Mak, T. W. *Cell* **2005**, *121*, 579–591.
- (5) Brown, G. C.; Borutaite, V. *Biochim. Biophys. Acta* **2008**, *1777*, 877–881.
- (6) Ripple, M. O.; Abajian, M.; Springett, R. *Apoptosis* **2010**, *15*, 563–573.
- (7) Takano, T.; Dickerson, R. E. *J. Mol. Biol.* **1981**, *153*, 79–94.
- (8) Jeng, W.-Y.; Chen, C.-Y.; Chang, H.-C.; Chuang, W.-J. *J. Bioenerg. Biomembr.* **2002**, *34*, 423–431.
- (9) Turner, D. L. *Eur. J. Biochem.* **1995**, *227*, 829–837.
- (10) Moon, S.; Patchkovskii, S. In *Calculation of NMR and EPR Parameters. Theory and Applications*; Kaupp, M., Bühl, M., Malkin, V. G., Eds.; Wiley: Weinheim, Germany, 2004.
- (11) Banci, L.; Bertini, I.; Luchinat, C.; Pierattelli, R.; Shokhirev, N. V.; Walker, F. A. *J. Am. Chem. Soc.* **1998**, *120*, 8472–8479.
- (12) Banci, L.; Bertini, I.; Rosato, A.; Varani, G. *J. Biol. Inorg. Chem.* **1999**, *4*, 824–837.
- (13) Marcus, R. A.; Sutin, N. *Biochim. Biophys. Acta* **1985**, *811*, 265–322.
- (14) Katki, H.; Weiss, G. H.; Kiefer, J. E.; Taitelbaum, H.; Spencer, R. G. S. *NMR Biomed.* **1996**, *9*, 135–139.
- (15) Dixon, D. W.; Hong, X.; Woehler, S. E. *Biophys. J.* **1989**, *56*, 339–351.